The 6th International Conference on Automotive Engineering (ICAE-6)
March 29 – April 2, 2010, BITEC, Bangkok, Thailand

Control of Inertial Stabilization Systems Using Robust Inverse Dynamics Control and Sliding Mode Control

Sangveraphunsiri V. and Malithong K.
Department of Mechanical Engineering, Faculty of Engineering,
Chulalongkorn University, Bangkok, Thailand

ABSTRACT

In this paper, we have designed controller to satisfy stabilization performance of an inertial stabilization system. This system has a 2-DOF gimbal which will be attached to an aviation vehicle. The camera is mounted at the center of the gimbals' inner joint. Motion control of gimbal is a difficult task, mainly because of the nonlinearities, dynamics modeling errors, friction and disturbances from the outside environment. A gimbaled stabilization system must stabilize the line of sight toward a target against the external motion induced by aerodynamic forces and aviation vehicle maneuvring. So, an advanced controller is needed. This paper shows a control method that brings together the nonlinear control and the line of sight (LOS) stabilization. In the low level part of the control, robust inverse dynamics control and sliding mode control are used in the inner loop or gimbal servo-system to control the gimbal motion. In the high level controller or the outer loop controller, indirect line of sight stabilization is a controller that maintains the sightline of a camera gimbal when it is subjected to external disturbances such as base motion. A tri-axial gyro is mounted on the base of the system to measure base rate and orientation of the gimbal in reference to the fixed reference frame. The experimental results confirm the validity of the control design procedures for the two-axis gimbaled stabilization system.

INTRODUCTION

At the present, many countries had developed radio control aircraft equipped with video camera and modern surveillance equipment and named "Unmanned Aerial Vehicle" or "UAV". The initial utilization has been progressing to useful role such as Reconnaissance, Surveillance, Search & Rescue and Telecommunications Relay. A camera gimbal is set up into the aircraft structure. Additionally, the motion of the camera can be controlled remotely from a ground station as well as the airplane.

An ordinary problem in inertial stabilization systems is the rejection of disturbances associated with moving components. Several techniques can be employed for controlling the gimbal motion. Li [2], [6] utilized a linear quadratic Gaussian (LQG) algorithm for modeling and compensating such disturbances in real time. Since the success of an LQG is often very dependent on the accuracy of the plant model. In practice, it is difficult to obtain the accurate dynamic model. So, several controllers were used instead. Lee [3] purposed a stable adaptive control, Li [5] purposed a self-turning controller, Ambrose [9] purposed a nonlinear robust control for a passive line-of-sight stabilization system. Ying [13] purposed Fuzzy logic control to control a laser tracking system (LTS) and Seong [12] using LQG/LTR Controller for a two-axis gimbal system.

Regional Center of Robotics Technology at Chulalongkorn University has been extending the capabilities of inertial stabilization systems for a number of years. Some Previous capabilities include researching for gimbal structure, gimbal kinematics, gimbal development, and the controller design [14]. This paper focuses on two controllers, the robust inverse dynamics control and the sliding mode control that takes advantage of robustness with respect to model uncertainties and disturbances, for stabilizing the servo loop.

GIMBAL DYNAMIC MODEL

The camera gimbal consists of two outer joints and two inner joints, Figure 1 (left). The outer joints, named the azimuth axis and the elevation axis respectively, both axes are controller by DC Servo motors. Two encoders measure the pan and tilt angles for the both axes. Inside the outer joints the camera is

mounted at the center of the inner joints. The inner joints have a freedom to move a few degrees and will prevent high frequency rotational vibrations to reach the cameras and causing blur in the images. This frame and the camera are kept at the center position by magnetic field, so that shock vibration will be damped out effectively.

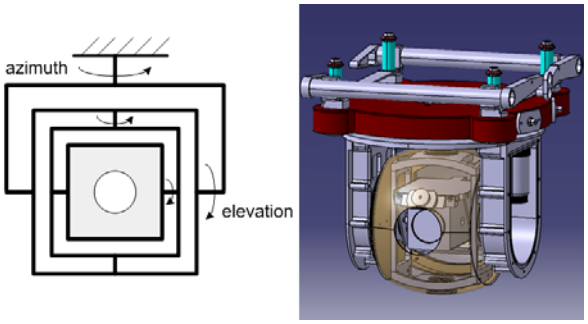

Figure 1: The two-axis gimbal configuration

The dynamic model of the two-axis gimbal can be written in the joint space, by using the Lagrange equation [14]. The friction force, $\mathbf{F}_s$, will be added to the dynamic equations, so the equation of motion in matrix form can be written as:

$$\mathbf{D}(q)\ddot{q} + \mathbf{C}(q,\dot{q})\dot{q} + \mathbf{F}_s \operatorname{sgn}(\dot{q}) + \mathbf{g}(q) = \tau \qquad (1)$$

In this expression, q is the vector of joint angles, τ is the torque vector applied to the joints, $\mathbf{D}(q)$ is the inertia matrix, $\mathbf{C}(q,\dot{q})$ is the vector of centripetal and Coriolis forces, $\mathbf{F}_s$ is an approximated friction forces. $\operatorname{sgn}(\dot{q}) = +1$ when $\dot{q}$ is positive and $\operatorname{sgn}(\dot{q}) = -1$ when $\dot{q}$ is negative. $\mathbf{g}(q)$ is the vector of gravitational forces and function. For this system, each matrix in the dynamic equations can be written as:

$$\mathbf{D}(q) = \begin{bmatrix} \mathbf{I}_{1_{22}} + \mathbf{I}_{2_{11}} \sin^2\theta_2 + \mathbf{I}_{2_{33}} \cos^2\theta_2 & 0 \\ 0 & \mathbf{I}_{2_{22}} \end{bmatrix}$$

$$\mathbf{C}(q,\dot{q}) = \begin{bmatrix} \frac{1}{2}\omega_2(\mathbf{I}_{2_{11}} - \mathbf{I}_{2_{33}})\times & \frac{1}{2}\omega_1(\mathbf{I}_{2_{11}} - \mathbf{I}_{2_{33}})\times \\ \sin(2\theta_2) & \sin(2\theta_2) \\ -\frac{1}{2}\omega_1(\mathbf{I}_{2_{11}} - \mathbf{I}_{2_{33}})\times & 0 \\ \sin(2\theta_2) & \end{bmatrix}$$

where $\mathbf{I}_{i_{jk}}$ is a member of row j and column k of moment of inertia of link i.

$$\mathbf{I}_1 = \begin{bmatrix} 0.065 & 0 & 0 \\ 0 & 0.069 & 0 \\ 0 & 0 & 0.07 \end{bmatrix},$$

$$\mathbf{I}_2 = \begin{bmatrix} 0.018 & 0 & 0 \\ 0 & 0.024 & 0 \\ 0 & 0 & 0.025 \end{bmatrix}$$

$\mathbf{I}_1$ and $\mathbf{I}_2$ can be obtained by computer aided design software.

THE CONTROLLER DESIGN

The controller structure is composed of two parts-the high level (outer loop) and the low level part (inner loop).

The high level controller has a goal, which is to hold or control the line of sight (LOS) of one object relative to another object or inertial space. In this paper, the LOS is the center of the field of view (FOV) of a camera. Two methods are implemented for inertial stabilizing the pointing vector defining the line of sight (LOS) of a two-axis gimbal [11]. The first, Direct LOS stabilization, with the angular rate sensors mounted on the LOS axes, is normally recommended for precision pointing applications. Gimbal size is impacted, since a larger payload volume is required to mount the sensors on the inner gimbal. With indirect LOS stabilization, currently being pursued for several applications, the rate sensors are mounted on the gimbal base. This can alleviate some of the problems associated with the direct stabilization approach. The disturbances, however, are not measured in the LOS coordinate frame, which can degrade performance.

From the constraints on hardware, we select the indirect LOS stabilization for the high level part. The indirect stabilization control configuration as shown in Figure 2 is used to control the overall system. A stabilizer or tri-axial gyro is mounted on the base of the system to measure base rate relative to the fixed earth reference frame. The base rate will be transformed to LOS coordinates. The outer loop controller, with angular rates and orientation information, is for cancellation of the disturbance due to motion of the airplane. It will compute commands to reject this disturbance.

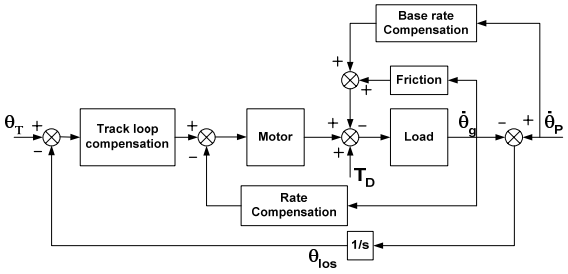

Figure 2: Indirect LOS Stabilization schematics

The low level part is the servo control loop or motion control. From the dynamic model, we allow the model to be imprecise. Model imprecision come from actual uncertainty about the plant (e.g., unknown plant parameters) or neglecting structural model. In the design of robust controllers for uncertain dynamical systems, the efforts have mainly been concentrated on two major approaches. The first one is based on the use of Lyapunov theory and assumes that the uncertainties satisfy a sufficient set of conditions called the "matching conditions". The second one is based on variable-structure systems theory and aims at driving the state trajectory of the system onto a switching surface in the state space and maintaining the trajectory on this surface for all subsequent time, thus establishing a so-called "sliding mode." It is well known that the sliding mode is governed only by the selected switching surface and, therefore, the state trajectory of the system is insensitive against uncertainties. The robust inverse dynamics control and the sliding mode control are two candidates for inner loop control of this system.

From Equation (1), this system is a nonlinear multivariable system. The controller technique called inverse dynamics control or nonlinear state feedback can be used to obtain the global linearization of the system dynamics. The dynamic equation of this system is expressed by Equation (1) which can be rewritten as

$$\tau = \mathbf{D}(q)\ddot{q} + \mathbf{N}(q,\dot{q}) \tag{2}$$

where $\mathbf{N}(q,\dot{q}) = \mathbf{C}(q,\dot{q})\dot{q} + \mathbf{F}_s \operatorname{sgn}(\dot{q}) + \mathbf{g}(q).$

Taking the control τ as a function of the system state in the form

$$\tau = \mathbf{D}(q)y + \mathbf{N}(q,\dot{q}) \tag{3}$$

Lead to the system can be described by:

$$\ddot{q} = y \tag{4}$$

where y represents a new input vector whose expression is to be determined yet. The nonlinear control law in Equation (3) is termed inverse dynamics control. This system under control Equation (3) is linear and decoupled with respect to the new input y. And y can be selected as:

$$y = \ddot{q}_d + K_P\tilde{q} + K_D\dot{\tilde{q}} + K_I\int_0^t \tilde{q}dt \tag{5}$$

where $q_d, \dot{q}_d, \ddot{q}_d$ are the desired joint trajectory, joint velocity, and joint acceleration. $\tilde{q} = q_d - q$. expresses the dynamics of position error, while tracking the given trajectory, $q_d, \dot{q}_d, \ddot{q}_d$. The gain K_P, K_D, K_I can be selected by specifying the desired speed of response. So, Equation (4) can be turned into the homogeneous differential equation as:

$$\ddot{\tilde{q}} + K_D\dot{\tilde{q}} + K_P\tilde{q} + K_I\int_o^t \tilde{q}dt = 0 \tag{6}$$

The block diagram of the inverse dynamics control is shown in Figure 3.

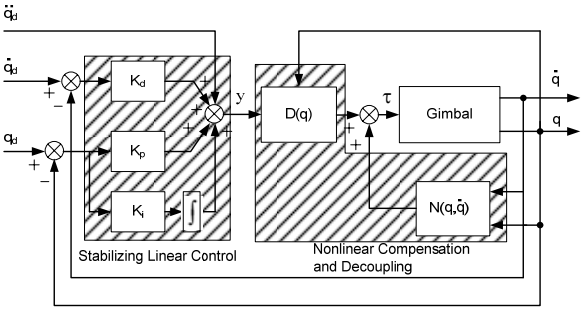

Figure 3: The block diagram of inverse dynamics control

From Equation (2), the control can be computed in real-time based on the parameters of the system dynamic model. In practice, it is difficult to obtain an accurate dynamic model especially in our case. Not only is the model inaccurate, but also the disturbances due to friction and environment change. The robust inverse dynamic and the sliding mode control will be used instead.

ROBUST INVERSE DYNAMICS CONTROL

Referring to the dynamic equation (Equation (3)), in the presence of uncertainties including modeling errors, unknown loads, and parameters measurement, the control vector is expressed by

$$\tau = \hat{\mathbf{D}}(q)y + \hat{\mathbf{N}}(q,\dot{q}) \tag{7}$$

where y is a new input vector to be determined, $\hat{\mathbf{D}}(q)$ and $\hat{\mathbf{N}}(q,\dot{q})$ denote the estimators of the inertial matrix $\mathbf{D}(q)$ and the nonlinear coupling matrix $\mathbf{N}(q,\dot{q})$ implemented in the controller, respectively.

Taking Equation (7) as a nonlinear control law gives

$$\mathbf{D}(q)\ddot{q} + \mathbf{N}(q,\dot{q}) = \hat{\mathbf{D}}(q)y + \hat{\mathbf{N}}(q,\dot{q}) \tag{8}$$

which allows the generation of

$$\begin{aligned}\ddot{q} &= y + \left(\mathbf{D}^{-1}(q)\hat{\mathbf{D}}(q) - \mathbf{I}\right)y + \mathbf{D}^{-1}\left(\hat{\mathbf{N}}(q,\dot{q}) - \mathbf{N}(q,\dot{q})\right) \\ &= y - \Gamma\end{aligned} \tag{9}$$

where $\mathbf{I}$ denotes a 3×3 identity matrix and

$$\Gamma = \left(\mathbf{I} - \mathbf{D}^{-1}(q)\hat{\mathbf{D}}(q)\right)y - \mathbf{D}^{-1}\left(\hat{\mathbf{N}}(q,\dot{q}) - \mathbf{N}(q,\dot{q})\right) \tag{10}$$

From Equation (9) can be rewritten as:

$$\ddot{q}_d - \ddot{q} = \ddot{q}_d - y + \Gamma \rightarrow \ddot{\tilde{q}} = \ddot{q}_d - y + \Gamma \tag{11}$$

Let define state variables as $\eta = \begin{bmatrix}\tilde{q} \\ \dot{\tilde{q}}\end{bmatrix}$

The state equation of Equation. (9) can be written as:

$$\begin{bmatrix}\dot{\eta} \\ \ddot{\eta}\end{bmatrix} = \begin{bmatrix}0 & \mathbf{I} \\ 0 & 0\end{bmatrix}\begin{bmatrix}\eta \\ \dot{\eta}\end{bmatrix} + \begin{bmatrix}0 \\ \mathbf{I}\end{bmatrix}\left(\ddot{q}_d - y + \Gamma\right) \tag{12}$$

In order to compensate for the uncertainties, the following input vector y is chosen:

$$y = \ddot{q}_d + K_D\dot{\tilde{q}} + K_P\tilde{q} + K_I\int_0^t \tilde{q}dt + w \tag{13}$$

The term w is an additional item to be designed to guarantee robustness to the effects of uncertainties described by Γ in Equation (10).

Substitute Eq. (13) into Eq. (12), we get:

$$\begin{bmatrix}\dot{\eta} \\ \ddot{\eta}\end{bmatrix} = \begin{bmatrix}0 & \mathbf{I} \\ 0 & 0\end{bmatrix}\begin{bmatrix}\eta \\ \dot{\eta}\end{bmatrix} + \begin{bmatrix}0 \\ \mathbf{I}\end{bmatrix}\left(-K_P\tilde{q} - K_D\dot{\tilde{q}} - K_I\int_0^t \tilde{q}dt - w + \Gamma\right)$$

$$\begin{bmatrix}\dot{\eta} \\ \ddot{\eta} \\ \dot{\beta}\end{bmatrix} = \begin{bmatrix}0 & \mathbf{I} & 0 \\ -K_P & -K_D & -K_I \\ \mathbf{I} & 0 & 0\end{bmatrix}\begin{bmatrix}\eta \\ \dot{\eta} \\ \beta\end{bmatrix} + \begin{bmatrix}0 \\ \mathbf{I} \\ 0\end{bmatrix}(\Gamma - w)$$

$$\dot{\zeta} = \mathbf{H}\zeta + \mathbf{G}(\Gamma - w) \tag{14}$$

where

$$\beta = \int_0^t \tilde{q}dt, \quad \zeta = \begin{bmatrix}\eta \\ \dot{\eta} \\ \beta\end{bmatrix}, \quad \mathbf{H} = \begin{bmatrix}0 & \mathbf{I} & 0 \\ -K_P & -K_D & -K_I \\ \mathbf{I} & 0 & 0\end{bmatrix},$$

and $\mathbf{G} = \begin{bmatrix}0 \\ \mathbf{I} \\ 0\end{bmatrix}$

For this system, ζ is a 6×1 vector. Since the matrices K_P, K_D and K_I are chosen so that $\mathbf{H}$ in Equation (14) is a Hurwitz matrix, i.e., $\mathbf{H}$ has all its eigen values with all negative real parts.

To determine w, consider the positive definite quadratic from Lyapunov function candidate.

$$V = \zeta^T\mathbf{Q}\zeta > 0 \qquad \forall\zeta \neq 0 \tag{15}$$

where $\mathbf{Q}$ is a symmetric positive definite matrix

$$\dot{V} = \dot{\zeta}^T\mathbf{Q}\zeta + \zeta^T\mathbf{Q}\dot{\zeta} \tag{16}$$

$$\dot{V} = \zeta^T\left(\mathbf{H}^T\mathbf{Q} + \mathbf{Q}\mathbf{H}\right)\zeta + 2\zeta^T\mathbf{Q}\mathbf{G}(\Gamma - w) \tag{17}$$

Because $\mathbf{H}$ has negative eigenvalues, any symmetric positive definite matrix P can be chosen to give a unique solution Q satisfying the relationship:

$$\left(\mathbf{H}^T\mathbf{Q} + \mathbf{Q}\mathbf{H}\right) = -\mathbf{P} \tag{18}$$

So, Equation (17) becomes:

$$\dot{V} = -\zeta^T\mathbf{P}\zeta + 2\zeta^T\mathbf{Q}\mathbf{G}(\Gamma - w) \tag{19}$$

To make $\dot{V}$ negative definite, we will need $\|w\| \geq \|\Gamma\|$. So, it will be true that:

$$w = \frac{\rho}{\left\|\mathbf{G}^T\mathbf{Q}\zeta\right\|}\left(\mathbf{G}^T\mathbf{Q}\zeta\right), \qquad \rho \geq \|\Gamma\| \tag{20a}$$

For small value of $\left\|\mathbf{G}^{\mathbf{T}}\mathbf{Q}\zeta\right\| < \varepsilon$, Eq. (20a) will be modified to:

$$w = \frac{\rho}{\varepsilon}\left(\mathbf{G}^{T}\mathbf{Q}\zeta\right), \qquad \left\|\mathbf{G}^{\mathbf{T}}\mathbf{Q}\zeta\right\| < \varepsilon \tag{20b}$$

The Equation (20b) is to prevent chattering.

Figure 4 shows the block diagram of the robust inverse dynamics control. An inertial measurement sensor is added to detect vehicle angular rate and orientation for outer loop control.

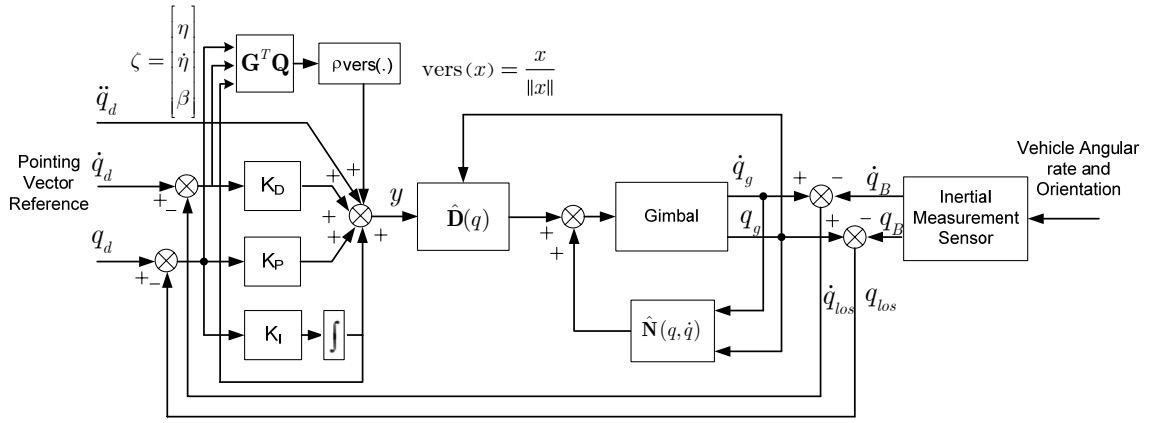

Figure 4: The block diagram of the robust inverse dynamics control

Then, the following state equations are obtained:

$$\dot{x}_1 = x_2 \tag{23}$$

$$\dot{x}_2 = \ddot{q} = \mathbf{D}^{-1}(x_1)\left[\tau - \mathbf{N}(x_1, x_2)\right] \tag{24}$$

$$= -\mathbf{D}^{-1}(x_1)\mathbf{N}(x_1, x_2) + \mathbf{D}^{-1}(x_1)\tau \tag{25}$$

where $\mathbf{N}(q,\dot{q}) = \mathbf{C}(q,\dot{q})\dot{q} + \mathbf{F}_s\,\mathrm{sgn}(\dot{q}) + \mathbf{g}(q)$

For existence and uniqueness of solution of above equation, assume that the functions $f(x)$ and $B(x)$ are continuous and sufficiently smooth.

The design of the sliding surface is presented below.

$$\sigma(x,t) = \begin{bmatrix}\sigma_1\\ \sigma_2\end{bmatrix} = G_1 e + G_2 \dot{e} = 0. \tag{26}$$

SLIDING MODE CONTROL

From dynamic equation (Equation (1)) can be written into state space form of a non-linear dynamic system.

$$\dot{x} = f(x) + B(x)u \tag{21}$$

The states are selected as the angular positions and their derivatives

$$x = \begin{bmatrix}x_1\\ x_2\end{bmatrix} = \begin{bmatrix}q\\ \dot{q}\end{bmatrix} \tag{22}$$

where $e = \begin{bmatrix}e_1\\ e_2\end{bmatrix} = \begin{bmatrix}q_{d1} - q_1\\ q_{d2} - q_2\end{bmatrix}$ is position error for each joint subsystem, The matrices G_1 and G_2 used in this design are

$$G_1 = \begin{bmatrix}c_{11} & 0\\ 0 & c_{22}\end{bmatrix}, \quad G_2 = \begin{bmatrix}1 & 0\\ 0 & 1\end{bmatrix}$$ where c_{11} and c_{22} are positive constants.

The derivation of the control involves the selection of a Lyapunov function $V(\sigma)$ and a desired form for $\dot{V}$, the derivative of the Lyapunov function. The selected Lyapunov function is

$$V = \frac{\sigma^T\sigma}{2} \tag{27}$$

For the system given by Equation (21), and the sliding surface given by Equation (26), a

sufficient condition for the existence of a sliding mode is that

$$\dot{V} = \sigma^T \dot{\sigma} < 0 \tag{28}$$

The derivative of the Lyapunov function will be negative definite, and this will ensure stability. A Stronger condition, guaranteeing an ideal sliding motion, is the η -reachability condition given by

$$\dot{V} = \sigma^T \dot{\sigma} < -\eta |\sigma| \tag{29}$$

where η is a strictly positive constant.

In a neighborhood of $\sigma = 0$, This is also a condition for reachability. It is desired that

$$\dot{V} = -\sigma^T K s\,g\,n(\sigma). \tag{30}$$

Where K is a positive-definite matrix. Thus, The last two equations together lead to

$$\sigma^T (K s\,g\,n(\sigma) + \dot{\sigma}) = 0 \tag{31}$$

A solution for the equation above is

$$\dot{\sigma} = -K\,\mathrm{sgn}(\sigma) \tag{32}$$

The expression for the derivative for the sliding function is

$$\dot{\sigma} = G_1 \dot{e} + \ddot{e} \tag{33}$$

$$\dot{\sigma} = G_1 \dot{e} + (\ddot{q}_d - \ddot{q}) \tag{34}$$

$$\dot{\sigma} = G_1 \dot{e} + \ddot{q}_d - \left(\mathbf{D}^{-1}(x_1)\tau - \mathbf{D}^{-1}(x_1)\mathbf{N}(x_1, x_2)\right) \tag{35}$$

Thus, from Equation (32) and Equation (35), we have that

$$\begin{aligned} -K s\,g\,n(\sigma) = {} & G_1 \dot{e} + \ddot{q}_d - \mathbf{D}^{-1}(x_1)\tau \\ & + \mathbf{D}^{-1}(x_1)\mathbf{N}(x_1, x_2) \end{aligned} \tag{36}$$

$$\begin{aligned} \tau = {} & \mathbf{D}(x_1)(G_1 \dot{e} + \ddot{q}_d) + \mathbf{N}(x_1, x_2) \\ & + \mathbf{D}(x_1) K s\,g\,n(\sigma) \end{aligned} \tag{37}$$

From Equation (37), the sliding mode control may cause a significant problem of chattering. The signum function in Equation (37) is changed by saturation function. This method can eliminate chattering effect of the control signal.

$$sat(\sigma_i) = \begin{cases} +1 & if \quad \sigma_i > \Phi_i \\ \dfrac{\sigma_i}{\Phi_i} & if \quad |\sigma_i| \le \Phi_i, \\ -1 & if \quad \sigma_i < -\Phi_i \end{cases} \tag{38}$$

Where $\Phi_i > 0$ is a switching boundary value in joint i .

Figure 5 shows the block diagram of the sliding mode control. An inertial measurement sensor is added to detect vehicle angular rate and orientation for outer loop control.

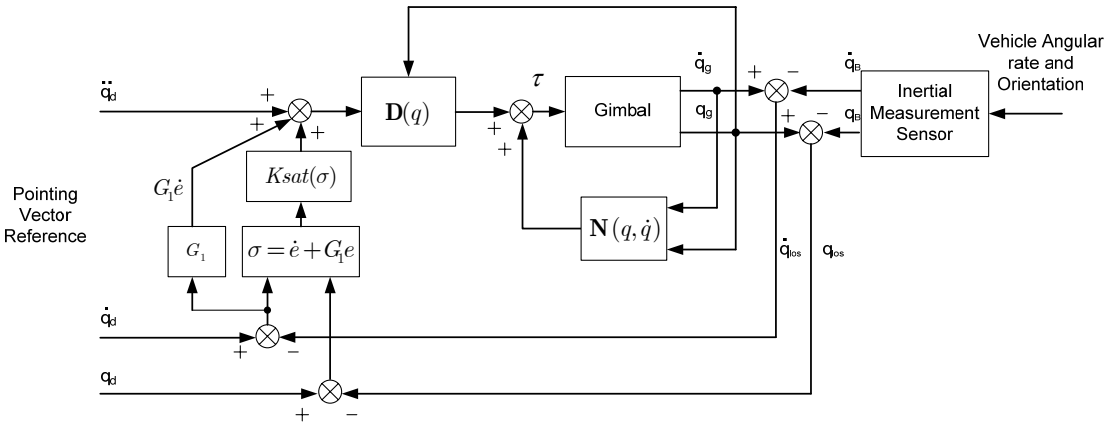

Figure 5: The block diagram of the sliding mode control

EXPERIMENT AND RESULT

EXPERIMENT METHOD

For the field work, the gimbal is mounted on the platform under the helicopter, as illustrated in Figure 6.

Figure 6: The gimbal mounted on the helicopter

Figure 7: Experimental and Environment Setup

In laboratory, the experimental setup is shown in Figure 7. The gimbal is hung freely on the trust frame, so that a base rate disturbance can be generated to emulate close to the real situation. A rate sensor is mounted on the base of the gimbal to detect the base rate and base orientation reference to the fixed reference frame. Robust inverse dynamics control and the sliding mode control with indirect LOS stabilization are implemented.

To demonstrate the performance of indirect LOS stabilization of two controllers mentioned in this paper, the system disturbances is generated by the angular motion of the base of the gimbal. The disturbance is added in two cases. First, the disturbance is added when the gimbal is pointing to the target. This case, the gimbal is shacked about 10 second and released while maintaining its LOS direction.

Second, the disturbance is added while the gimbal is moving to the new target. To test the tracking capability, the reference trajectory $q_d, \dot{q}_d, \ddot{q}_d$ is generated from the trapezoidal velocity profile or s-profile trajectory. The gimbal is swung to generate the slew motion to create the environment motion close to the real situation. A trapezoidal velocity profile is generated by setting traveling distance, maximum velocity, and maximum acceleration equal to 1 rad, 0.5 rad/sec, and 0.8 rad/sec2 respectively.

RESULTS

For the first case, the disturbance is added when the gimbal is pointing to the target or maintaining the same position. The gimbal is shacked about 10 second and released while maintaining its LOS direction. The response of azimuth and pitch angle for robust inverse dynamic and sliding mode control are shown in Figure 8 - 11, respectively. They display the LOS stabilized performance under the disturbance of random signal (Blue line).

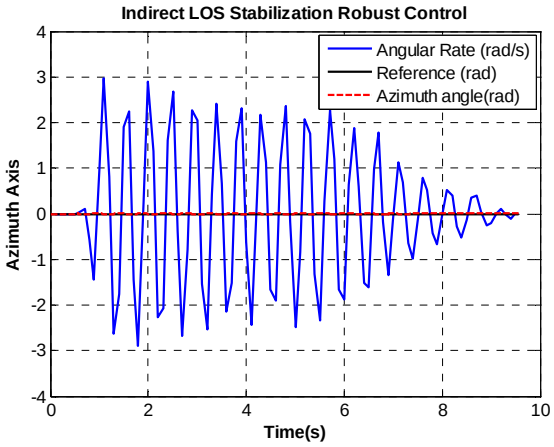

Figure 8: The response of robust inverse dynamics control for vibrating of the azimuth angle.

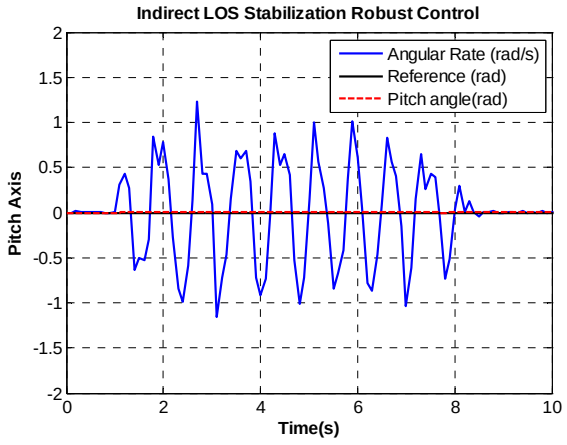

Figure 9: The response of robust inverse dynamics control for vibrating of the pitch angle.

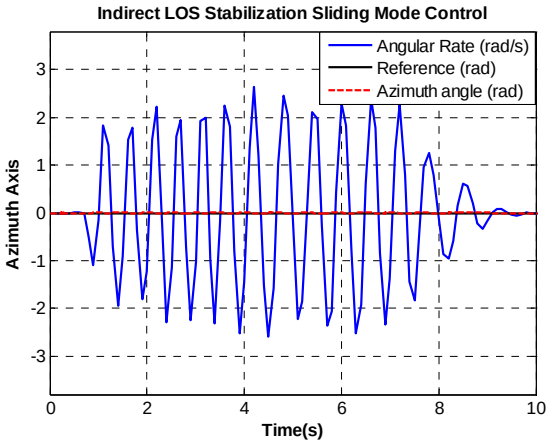

Figure 10: The response of sliding mode control for vibrating of the azimuth angle.

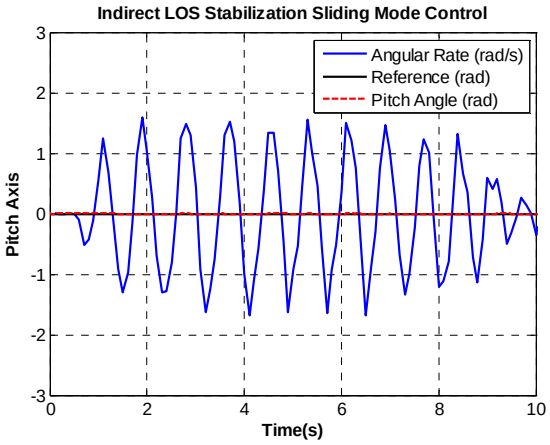

Figure 11: The response of sliding mode control for vibrating of the pitch angle.

The second case, the controller must be tracking the input and rejecting the base rate disturbance at the same time. The disturbance is in the form of shaking the base. The response of azimuth and pitch angle for robust inverse dynamic and sliding mode control are shown in Figure 12 - 15, respectively. They display the LOS stabilized performance for s-profile trajectory under the disturbance of random signal (Blue line). The experimental results show that the robust inverse dynamics control and the sliding mode control perform very effective for our inertial stabilization system, and are very promising controllers.

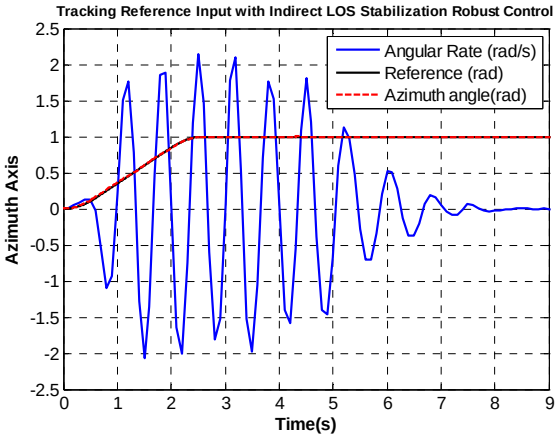

Figure 12: The response of robust inverse dynamics control for tracking of the azimuth angle.

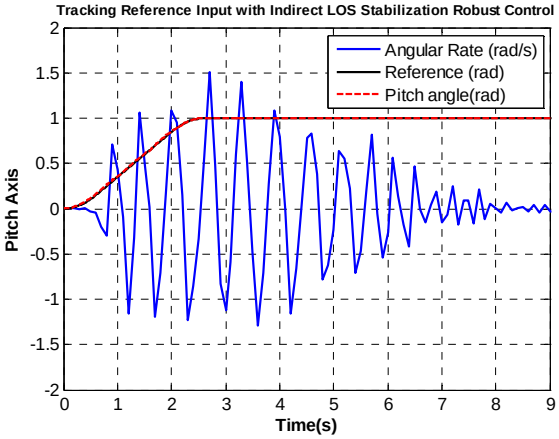

Figure 13: The response of robust inverse dynamics control for tracking of the pitch angle.

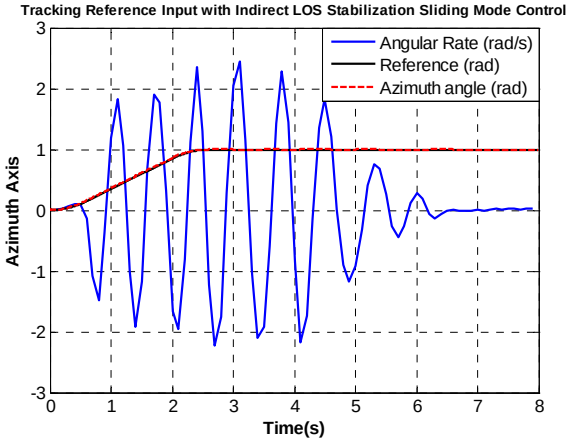

Figure 14: The response of sliding mode control for tracking of the azimuth angle.

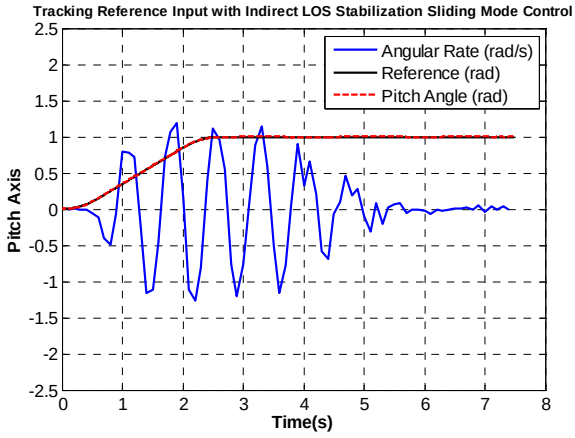

Figure 15: The response of sliding mode control for tracking of the pitch angle.

CONCLUSION

In this paper, we have designed controllers to satisfy stabilization performance of a two-axis gimbal system. The details of the two controllers, the robust inverse dynamic and the sliding mode control, are described. The robust inverse dynamic and the sliding mode control can be used for trajectory tracking in the presence of dynamics uncertainties. Indirect stabilization is reducing the jittering due to base rate disturbances. Unbalanced mass and friction can also be compensated by integral action. The experiment results in the two-axes gimbal are presented to verify the effectiveness of the proposed method in rejecting carrier disturbances. The controllers perform very effective for this system.

REFERENCES

1. C. M and Hamel, J.F., 1994. The agile eye: a high-performance three-degree-of-freedom camera-orienting device, Robotics and Automation, Proceedings of the IEEE.
2. B. Li, 1994. Identification and compensation for Coulomb friction in stochastic systems, Ph.D. dissertation, Univ. Texas-Arlington
3. Lee T.H., Koh E.K., Loh M.K., 1996. Stable adaptive control of multivariable servomechanisms, with application to a passive line-of-sight stabilization system, IEEE Transactions on Industrial Electronics, Volume: 43, Issue: 1, Feb. 1996, 98 – 105
4. Li B., Hullender D. and DiRenzo M., 1998. Nonlinear Induced Disturbance Rejection in Inertial Stabilization Systems, IEEE Transactions on control systems technology, Vol. 6, No.3, May 1998
5. Li B. and Hullender D., 1998. Self-Tuning Controller for Nonlinear Inertial Stabilization System, IEEE Transactions on control systems technology, Vol. 6, No.3, May 1998.
6. Li B., Hullender D., and DiRenzo M., 1998. Nonlinear induced disturbance rejection in inertial stabilization systems, IEEE Trans. Contr. Syst. Technol., vol. 6, no. 3, May 1998.
7. Becker G., Cubalchini R., Tham Q. and Anagnost J., 1999. Generation of Structural Design Constraints for Spaceborne Precision Pointing System, Proceedings of the 2001 IEEE International Conference on Control Applications, August 1999, Hawaii, USA.
8. Erbatur K., Kaynak 0. and Sabanovic A., 1999. A Study on Robustness Property of Sliding-Mode Controllers: A Novel Design and Experimental Investigations, IEEE Transactions on industrial electronics, Vol. 46, No.5, May 1999.
9. Ambrose H., Qu Z. and Johnson R., 2001. Nonlinear Robust Control For A Passive Line-of-Sight Stabilization System, Proceedings of the 2001 IEEE International Conference on Control Applications, September 5-7, 2001, Mexico.
10. Yoon S. and Lundberg J. B., 2001. Equations of Motion for a Two-Axes Gimbal System, IEEE Transactions on Aerospace and Electronic system, Vol. 37, No.3, July 2001.
11. Kenady P. J., 2003. Direct Versus Indirect Line of Sight (LOS) Stabilization, IEEE Transactions on control systems technology, Vol. 11, No.1, January 2003
12. Bai Y.; Zhuang H. and Roth Z.S., 2005. Fuzzy logic control to suppress noises and coupling effects in a laser tracking system Control Systems Technology, IEEE Transactions on Volume 13, Issue 1, Jan. 2005, 113 – 121
13. Seong K. J., Kang H., Yeo, B. and Lee, H., 2006. The Stabilization Loop Design for a Two-Axis Gimbal System Using LQG/LTR Controller , SICE-ICASE, International Joint Conference 18-21 Oct. 2006, 755 – 759
14. Wongkamchang P., Sangveraphunsiri V., 2008. Control of Inertial Stabilization Systems Using Robust Inverse Dynamics Control and Adaptive Control., The Thammasat International Journal of Science and Technology, 2008, Volume 13, No. 2, 20 – 32.
15. Slotine J.-J.E., 1987. Robust Control of Robot Manipulators, Int. J. Robotics Research.

16. Craig J.J., 1989. Introduction to Robotics mechanics and control, 2nd edition, Silma, Inc.
17. Slotine J.-J.E. and Li W., 1991. Applied Nonlinear Control, ISBN 0-13-040049-1, Prentice -Hall International, Inc., New Jersey.
18. Edward C. and Spurgeon S.K., 1998. Sliding Mode Control: Theory and Applications, T.J. International Ltd, Padstow, UK